Efficient synthesis of ammonia from N_2 and H_2 alone in a ferroelectric packed-bed DBD reactor

2015 Plasma Sources Sci. Technol. 24 065011

(http://iopscience.iop.org/0963-0252/24/6/065011)

IOP Publishing Plasma Sources Science and Technology

Plasma Sources Sci. Technol. **24** (2015) 065011 (7pp) doi:10.1088/0963-0252/24/6/065011

Efficient synthesis of ammonia from N_2 and H_2 alone in a ferroelectric packed-bed DBD reactor

A Gómez-Ramírez[1], J Cotrino[1,2], R M Lambert[1,3] and A R González-Elipe[1]

[1] Laboratory of Nanotechnology on Surfaces. Instituto de Ciencia de los Materiales de Sevilla (CSIC-Universidad de Sevilla), Avda. Américo Vespucio 49, 41092 Sevilla, Spain
[2] Departamento de Física Atómica, Molecular y Nuclear, Universidad de Sevilla, Avda. Reina Mercedes, 42022 Sevilla, Spain
[3] Chemistry Department, Cambridge University, Cambridge CB2 1EW, UK

E-mail: anamaria.gomez@icmse.csic.es

Received 11 June 2015, revised 2 October 2015
Accepted for publication 12 October 2015
Published 3 November 2015

Abstract

A detailed study of ammonia synthesis from hydrogen and nitrogen in a planar dielectric barrier discharge (DBD) reactor was carried out. Electrical parameters were systematically varied, including applied voltage and frequency, electrode gap, and type of ferroelectric material ($BaTiO_3$ versus PZT). For selected operating conditions, power consumption and plasma electron density were estimated from Lissajous diagrams and by application of the Bolsig + model, respectively. Optical emission spectroscopy was used to follow the evolution of plasma species (NH*, N*, N_2^+ and N_2^*) as a function of applied voltage with both types of ferroelectric material. PZT gave both greater energy efficiency and higher ammonia yield than $BaTiO_3$: 0.9 g NH_3 kWh^{-1} and 2.7% single pass N_2 conversion, respectively. This performance is substantially superior to previously published findings on DBD synthesis of NH_3 from N_2 and H_2 alone. The influence of electrical working parameters, the beneficial effect of PZT and the importance of controlling reactant residence time are rationalized in a reaction model that takes account of the principal process variables

Keywords: ammonia production, plasma assisted catalysis, ferroelectric moderator, dielectric barrier discharge

S Online supplementary data available from stacks.iop.org/PSST/24/065011/mmedia

(Some figures may appear in colour only in the online journal)

1. Introduction

The industrial scale catalytic synthesis of ammonia from N_2 and H_2 is carried out at high temperatures and pressures by means of the Haber-Bosch process, using iron-based catalysts [1]. Due to its global importance, especially with respect to food production, much effort has been devoted over decades to improve the energy efficiency and operational requirements of the process [2–7]. Plasma synthesis of ammonia has been investigated as a potential alternative method that can be operated under less extreme conditions and in a distributed mode. Microwave plasmas [8–10], microdischarges [11] and arc plasmas [12] have been used for this purpose, though a major drawback is the very small ammonia yield and low energy efficiency of these methods, generally operated at low pressures. Recently, atmospheric pressure dielectric barrier discharge (DBD) plasmas have been reported to produce ammonia yields in the order of 2%, for example by Mizushima *et al* [13, 14], using a catalyst-loaded membrane as dielectric material, by Hong *et al* [15] using a DBD packed bed reactor filled with dielectric spheres and by Bai *et al* [16].

Commonly used DBD reactors have a fixed cylindrical geometry which allows little flexibility for testing the influence of electrode gap or the size and shape of the

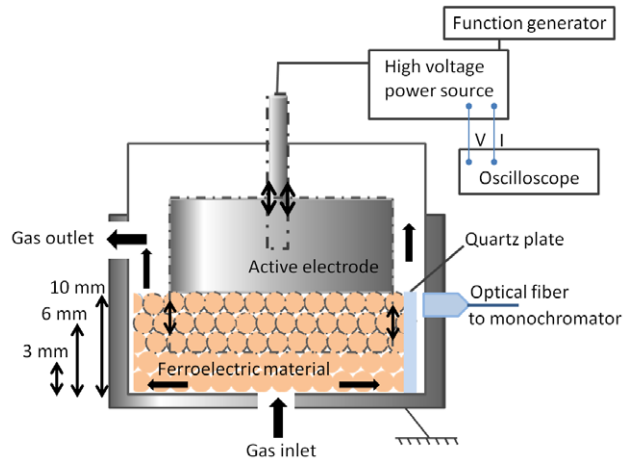

Figure 1. Schematic of parallel plate reactor set-up.

inter-electrode material on process performance. Herein we report on the plasma synthesis of ammonia in a ferroelectrically-moderated DBD parallel plate reactor. In addition to investigating the effects of applied voltage and frequency, the consequences of varying the inter-electrode gap and the type of ferroelectric material in the inter-electrode space have also been examined. Previous work by ourselves and by others using fixed geometry cylindrical DBD reactors showed that filling the inter-electrode gap with pellets of a ferroelectric material enabled a substantial decrease in operating voltage and hence an increase in the overall energy efficiency of the process [17–20]. Here we report on the effect of two ferroelectric materials, $BaTiO_3$ and PZT, known for their different high permittivities and Curie temperatures, on the synthesis of ammonia from nitrogen and hydrogen alone—i.e. in the absence of any added inert gas. It is shown that PZT yields higher ammonia production than $BaTiO_3$ and that by optimizing operational conditions a single pass yield of ammonia of 2.7% with respect to the nitrogen feed may be achieved. To our knowledge, this reaction yield exceeds anything previously reported for plasma synthesis of NH_3 from N_2 and H_2 alone under ambient conditions. Moreover it approaches that delivered by the Haber process (15% [1]) under far more extreme conditions. Our findings, including a study of the evolution of the plasma-excited species by optical emission spectroscopy (OES) and determination of the electron density by means of the Bolsig + model [21], provide fundamental clues to the mechanism of plasma synthesis of ammonia and signpost avenues for future progress.

2. Experimental section

2.1. Reactor configuration, electrical characterization and plasma diagnosis

The stainless steel DBD reactor (figure 1) incorporated two parallel electrodes separated by a variable gap filled with pellets of a ferroelectric material. The active electrode, supported on the ferroelectric bed, was connected to a high voltage power supply by means of a feed-through, while the bottom wall of the reactor acted as grounded electrode. The inter-electrode

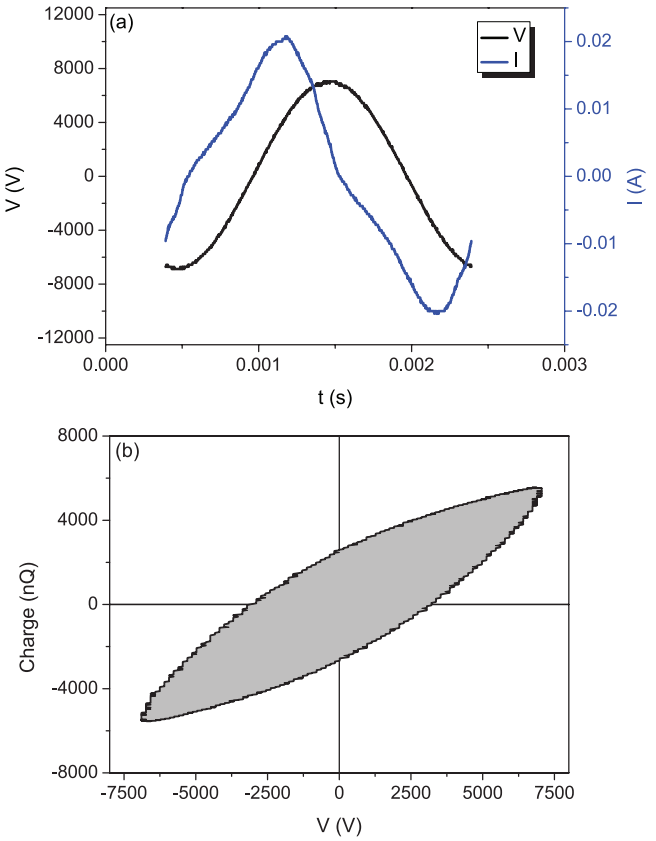

Figure 2. (a) Plots of $I(t)$ and $V(t)$ for a 10 mm inter-electrode gap. N_2:H_2 = 1 : 1, total flow rate 38.3 sccm, PZT as ferroelectric moderator. (b) The corresponding Lissajous curve.

gap could be varied by using different amounts of ferroelectric material between the active and ground electrodes. All experiments were carried out at atmospheric pressure and without external heating. The maximum reactor temperature during operation was 50 °C.

A function generator (Stanford Research System, Model DS345) and a high voltage power supply (Trek, Model 20/20 C) were used to power the reactor. Process performance was analysed by varying both the voltage and the frequency of the input power and characteristic intensity $I(t)$ and voltage $V(t)$ curves were recorded by means of an oscilloscope (Tektronix TDS2001C) directly connected to the high voltage power supply, which incorporated a high voltage probe and a series resistance. The power consumed P(W) within the plasma was determined from the corresponding Lissajous diagrams [22]. The values obtained agreed with those determined from power calculations based on one period integration of the product $I(t)\cdot V(t)$; figure 2 shows representative I–V and Lissajous curves. Energy efficiency is expressed as amount of ammonia produced (grams) per consumed unit of energy, (kWh). Where appropriate, the absolute flow rate is also indicated.

In high pressure discharges the electron density can be expressed as $n_e = J/(e^*\mu_e^*E)$ (equation (1)), where e is the electron charge, E the electric field and J the macroscopic current density, both of them estimated from the characteristic I–V curves and the latter calculated by considering the total electrode area. μ_e is the electron mobility obtained by

applying the Bolsig + model [21]. This model provides a numerical solution to the Boltzmann equation for electrons in weakly ionized gases constrained within an uniform electric field, conditions that are typical for collisional low-temperature plasmas. In this way the electron densities calculated using equation (1) are in reality a minimum limit for the actual electron densities in the zones occupied by the plasma in the inter-electrode gap space.

Emission spectra (Avantes, AvaSpec DUAL) were acquired via an optical fibre feedthrough situated in the lateral wall of the reactor with the probe tip placed as near as possible to the plasma region (figure 1). The monochromator resolution was 0.3 nm.

2.2. Gas delivery and product reaction analysis

N_2 and H_2 (Air Liquide) were delivered through a diffuser inlet situated in the centre of the grounded electrode, to promote uniform gas residence time in the plasma zone. Gas flow rates were controlled by means of mass flow controllers (Bronkhorst, EL-flow type) and the exit gas was delivered to a mass spectrometer (Sensorlab, Prima Plus − Pfeiffer Vacuum). Measurements were carried out with N_2:H_2 mixtures of 1 : 1, 1 : 2, 1 : 3, 1 : 4, 1 : 5 and 1 : 6 and the residence time of gases within the plasma region was constant in all the experiments (17.5 s), unless otherwise specified in the text.

2.3. Ferroelectric material

The inter-electrode space of the reactor was filled with $BaTiO_3$ or PZT pellets. The former was supplied in the form of pellets by Catal. International Ltd whereas PZT pellets were prepared in our laboratory by pressing and sintering powder supplied by APC International Ltd. The latter procedure, described in detail in [23], provided good consistency and optimum control over the pellet size distribution. The dielectric constant of $BaTiO_3$ varies from 1250 to 10 000 over the temperature range 20 − 120 °C, while that of PZT is ~1900 with a Curie point of 360 °C, far higher than the working temperature of the reactor. The BET surface area of both kinds of ferroelectric material was very similar, 0.74 m^2 gr^{-1} and 0.71 m^2 gr^{-1} for PZT and $BaTiO_3$, respectively. The pellet size was ~1.5 mm for experiments carried out with inter-electrode gaps of 3 and 6 mm, and ~3 mm for experiments performed with a gap of 10 mm.

3. Results and discussion

In order to optimize ammonia production, a systematic investigation of the influence of experimental parameters on the reaction yield and energy efficiency of the process was carried out as described below.

3.1. Effect of reaction mixture

Previous studies indicated that the reaction efficiency depends on the nitrogen to hydrogen ratio in the reactant mixture [8, 13, 14] and a similar behaviour was found under our conditions. As illustrated in figure 3, for both types of ferroelectric material, N_2:H_2 gas mixtures in the range 1 : 3 to 1 : 1 provided the maximum energy efficiency; higher N_2:H_2 ratios resulted in a sharp decrease in ammonia production. Maximum energy efficiencies of 0.28 g NH_3 kWh^{-1} and 0.44 g NH_3 kWh^{-1}, respectively, for $BaTiO_3$ and PZT were found, that of PZT always being the higher of the two. Thus PZT is a substantially more effective moderator and catalyst than $BaTiO_3$.

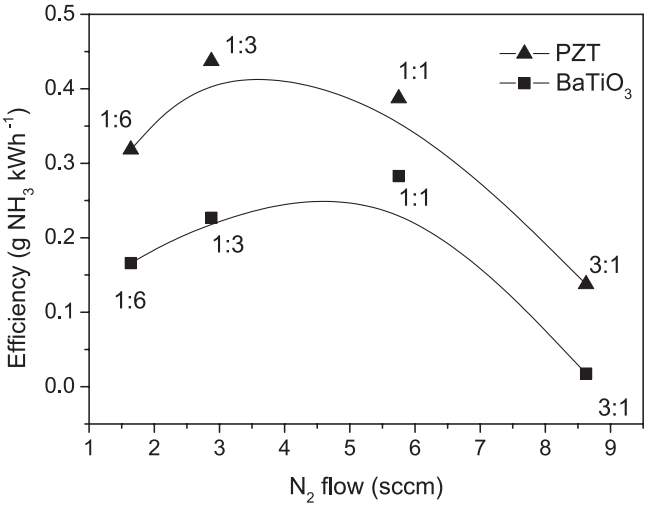

Figure 3. Ammonia production efficiency referred to input nitrogen flow for different gas mixtures (N_2:H_2) and ferroelectric materials. Total flow rate constant (11.5 sccm) and independent of N_2:H_2 ratio. Operating conditions: 3 mm gap, pellet size ~1.5 mm. 500 Hz and 3 kV.

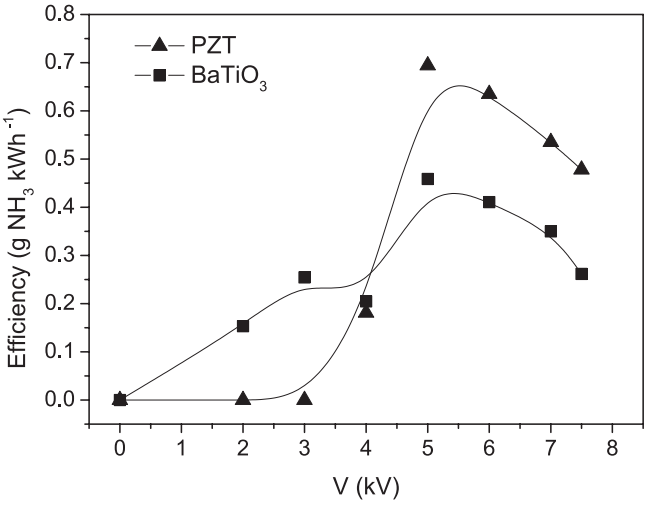

Figure 4. Efficiency versus applied voltage for PZT and $BaTiO_3$ as ferroelectric materials. Electrical operating conditions are given in the text. N_2:H_2 ratio 1 : 1.

3.2. Ferroelectric material and electrical operating conditions

Figure 4 shows the typical dependence of energy efficiency on applied voltage for an inter-electrode gap of 10 mm and a frequency of 500 Hz. With both ferroelectric materials, the efficiency exhibited a maximum at 5.5 kV, more pronounced

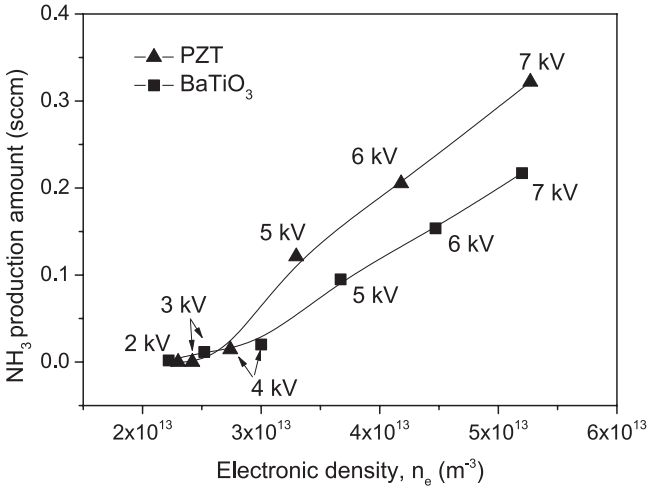

Figure 5. Ammonia yield as a function of calculated plasma electron density for different applied voltages at 500 Hz. Inter-electrode gap 10 mm and N_2:H_2 = 1 : 1.

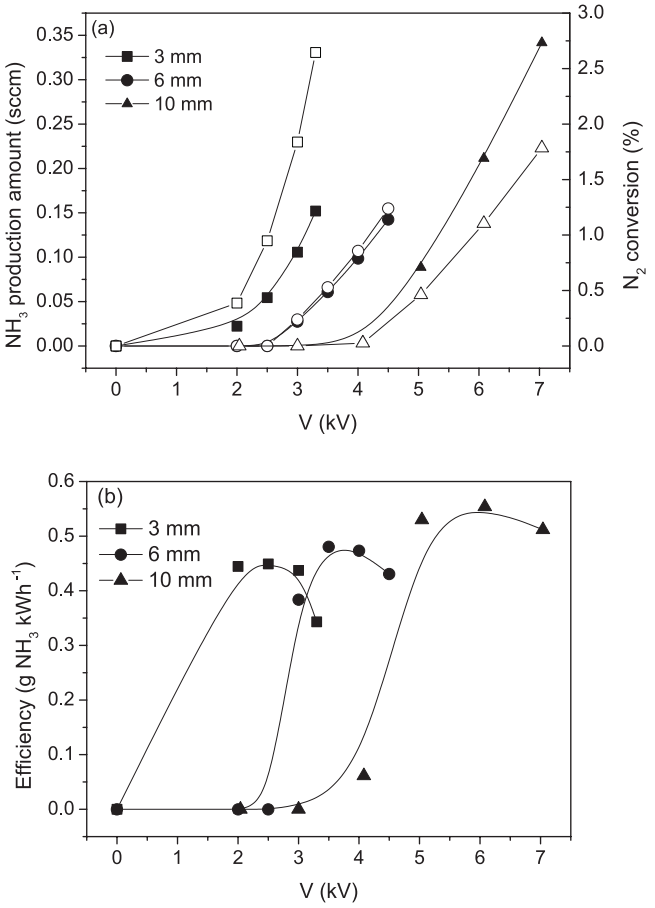

Figure 6. (a) Ammonia production (filled symbols) and N_2 conversion (unfilled symbols). (b) Process energy efficiency as a function of applied voltage for three different inter-electrode gaps. Frequency 500 Hz and N_2:H_2 = 1 : 3.

in the case of PZT, which material also showed a threshold voltage for plasma ignition. At constant current, the energy efficiency decreased as frequency increased, but the effect was small over the range 500–4000 Hz, being most noticeable, though minor, at low NH_3 production (for example, for 1 : 6 or 3 : 1 gas proportions, see figure 3).

The markedly higher energy efficiency obtained with PZT may be associated at least in part with the higher associated plasma electron density, as illustrated in figure 5 which shows that for comparable electron densities, ammonia production was always significantly higher when using PZT. It must be stressed that the calculated electron densities used in figure 5 can only be used for comparative purposes since, as deduced from the method utilized for their determination (see experimental section), they underestimate the actual values of this parameter in the plasma activated regions in the inter-electrode gap.

3.3. Effect of inter-electrode gap

Use of a parallel plate reactor enabled variation of the inter-electrode gap, a parameter that proved to be critical in controlling both the ammonia yield and the energy efficiency of the system. Figure 6(a) shows the dependence of ammonia production and % nitrogen conversion on the applied voltage for three different inter-electrode gaps of 3, 6 and 10 mm with N_2:H_2 = 1 : 3, using PZT as ferroelectric and a frequency of 500 Hz. Figure 6(b) shows the corresponding data for energy efficiency. Similar results were obtained with $BaTiO_3$ (see supporting information S1) although in that case the overall yield was smaller, in line with the results presented in figures 3 and 4. In every case ammonia production and N_2 conversion increased sharply with voltage, reaching limiting values of 0.34 sccm and 2.7% for inter-electrode gaps of 10 and 3 mm, at 7 and 3.3 kV respectively. It is important to note that the maximum applied voltages and associated chemical conversions shown in figure 6(a) were limited by the characteristics of the power supply. Extrapolation of these data suggests that a more powerful voltage source could have produced much higher ammonia yields: this aspect is the subject of further study.

The energy efficiency of the system attained its maximum value with the 10 mm gap at 6 kV. The similar shape of the three efficiency curves shown in figure 6(b) indicates that there exist well-defined voltage-current values for which the efficiency is maximized; it is possible that the decrease in efficiency observed at the highest voltages is due to destruction of initially-formed ammonia. Although the maximum energy efficiencies were similar (0.45, 0.48 and 0.55 g NH_3 kWh^{-1} for the 3, 6 and 10 mm gaps, respectively) the N_2 conversion increased with decreasing inter-electrode gap (2.7% and 1.8% for the 3 mm and 10 mm gaps, respectively). This is simply the consequence of having to increase the gas flowrate as the inter-electrode gap increased, in order to maintain constant residence time: the increment in N_2 flow was not balanced by the increment in NH_3 production, so N_2 conversion necessarily decreased.

3.4. Residence time

Changing the residence time of the reaction mixture within the reactor at constant N_2:H_2 composition had little effect on

the electrical working parameters of the system. It did however have a large effect on the overall energy efficiency. Here, the specific energy (input power divided by gas flow rate) increased with residence time. Whereas with respect to energy efficiency, as defined above, the shorter the residence time, the higher the energy efficiency, especially when using PZT as moderator. For example, with PZT at 500 Hz and 3 kV and N_2:$H_2 = 1:3$ and a 3 mm gap, halving the residence time from 17.5 s to 8.8 s increased the efficiency from 0.44 to 0.9 g NH_3 kWh^{-1}. The latter value is more than twice the previously reported best value for a DBD packed bed reactor [15] (0.39 g NH_3 kWh^{-1}). This increased energy efficiency resulted from both a higher production of ammonia and a lower power consumption (N_2 conversion varied from 1.83% at 17.5 s to 1.38 % at 8.8 s).

With $BaTiO_3$ as ferroelectric the effects of residence time were similar, although much less pronounced than with PZT. For example with N_2:$H_2 = 1:1$ the efficiency increased from 0.28 to only 0.31 g NH_3 kWh^{-1} upon halving the residence time. These results indicate that (i) secondary reactions that lead to the destruction of initially formed ammonia become increasingly important at longer residence times and (ii) in addition to improving the electrical characteristics of the system, as does $BaTiO_3$, PZT plays a specific catalytic role in NH_3 production.

It is noteworthy that the best performance we achieved with PZT (2.7% N_2 conversion) is substantially superior to anything previously reported for ammonia synthesis from nitrogen and hydrogen alone, by means of DBD; see for example [13, 14]. Although Hong *et al* [15] achieved higher N_2 conversion (4.2%), this required the use of 14% Ar as carrier gas, which on grounds of cost would be entirely unsuited to large scale production, which of course is the only practical goal of ammonia synthesis. Finally, while Bai *et al* [16] obtained a higher energy efficiency than we did by using a micro-DBD reactor (1.83 g NH_3 kWh^{-1}), the conversion they archived was only 1.25 %.

3.5. Plasma diagnosis and reaction mechanism

Figure 7 shows a series of OE spectra recorded in the range 275 to 450 nm as a function of discharge operating voltage under similar conditions to those used for obtaining the data shown in figure 4 (10 mm gap, 500 Hz) with PZT as ferroelectric moderator. The spectral assignments are as follows: second positive system of nitrogen [$C^3\Pi \rightarrow B^3\Pi$] (357.9 nm), first negative system of N_2^+, [$B^2\Sigma_u^+ \rightarrow X^2\Sigma_g^+$] (391.4 nm) and the transition [$A^3\Pi \rightarrow X^3\Sigma$] corresponding to excited NH^* species (336 nm) [15, 24, 25]. (Note that N_2^* exhibits strong emission at 337 nm, close to the 336 nm NH^* emission, from which it is distinguishable in the spectra. In order to improve the reliability of the normalization described below, we therefore used the 357.9 nm line to follow N_2^*). In addition a well-defined line at 1011.5 nm corresponding to excited atomic nitrogen N^* was also observed [26]. No lines due to atomic hydrogen could be detected (to the best of our knowledge, there are no examples of published work in which emission from atomic H was detected in H_2-containing packed-bed DBDs operated under conditions of gas composition and electrical parameters similar to ours).

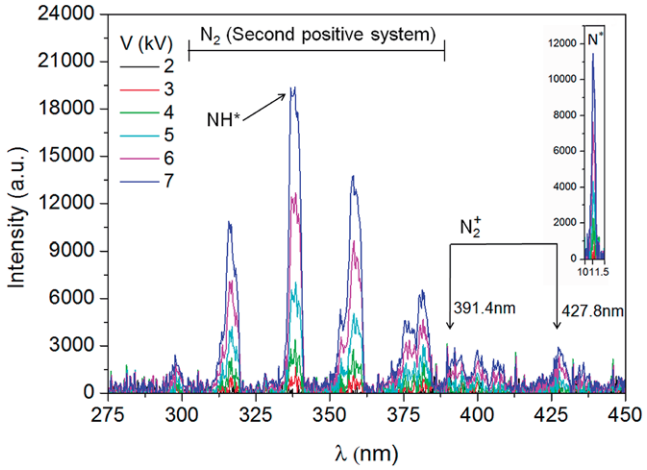

Figure 7. Time averaged optical emission spectra recorded at different operating voltages with PZT as ferroelectric material.

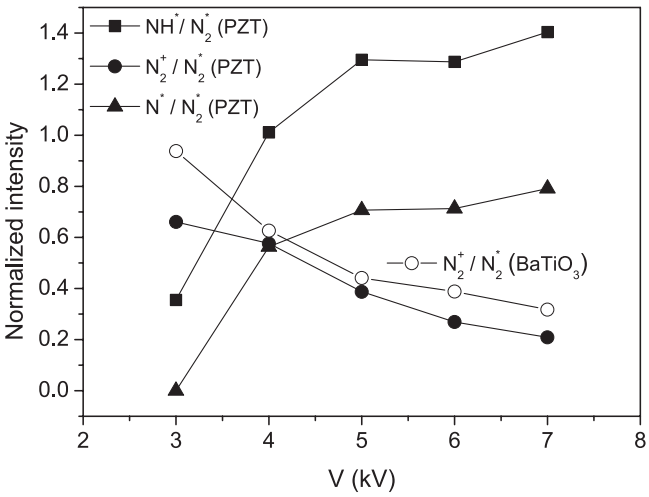

Figure 8. Relative intensity of selected emission bands as a function of applied voltage using PZT as plasma moderator. N_2^+/N_2^* relative intensity observed with $BaTiO_3$ shown for comparison; see also supporting information figure S2.1 (stacks.iop.org/PSST/24/065011/mmedia).

All spectral intensities increased with operating voltage. However, whereas the relative intensities of the NH^* and N^* emission normalized to that of N_2^* increased with voltage, the normalized intensity of the N_2^+ emission showed the opposite behaviour, *decreasing* as voltage increased (figure 8) and ammonia production *increased* (figure 6(a)). Assuming that the ratio between band intensities is equivalent to that between the concentration of the emitting species, this indicates that N_2^+ plays a key role in the overall process and the implication of these findings in regard to possible reaction mechanisms is discussed below. For comparison, a plot of the N_2^+/N_2^* relative intensity with $BaTiO_3$ as moderator is included in figure 8 (the relative intensities of the other emission lines are shown in the supporting information—their observed variation was similar to that found for PZT.)

3.6. Mechanism of ammonia formation

It has been proposed that plasma synthesis of ammonia from nitrogen and hydrogen involves N_2^+ ions as initiators and NH radicals as intermediates [11, 13, 15, 16], and indeed our OES data confirm that these species are present in the plasma, along with N*. A plausible and thermochemically feasible mechanism that accords with observation may be tentatively proposed, as shown below. (Kinetic modelling studies that are beyond the scope of the present paper are in hand.)

$$N_2 + e^- \rightarrow N_2^* + e^- \quad (1)$$

$$N_2^* + N_2^* \rightarrow N_2^+ + N_2 + e^- \quad (2)$$

$$N_2 + e^- \rightarrow N_2^+ + 2e^- \quad (3)$$

$$N_2 + e^- \rightarrow N^* + N + e^- \quad (4)$$

$$N^* + H_2 \rightarrow NH + H \quad (5)$$

[27] (gas and/or surface reaction).

N_2^+ is formed by direct electron impact or by collision between metastable states of nitrogen [8]. The reactions (2, 3) that generate the reactive initiator N_2^+ would thus contribute to control of the rate of the overall process.

The opposite dependences on discharge voltage observed for ammonia formation and N_2^+ concentration (figures 6(a) and 8 respectively) suggest that important gas phase and heterogeneous channels for NH formation are:

$$N_2^+ + H_2 \rightarrow NH + \text{product} \quad (6)$$

$$N_2^+ + 2\,H\,(\text{adsorbed}) \rightarrow NH\,(\text{adsorbed}) + \text{product} \quad (7)$$

In regard to reaction (7), it is noteworthy that other authors have attributed plasma-induced formation of radicals to catalytic effects occurring at reactor walls [28–30]. In the present case the plasma-exposed surfaces are dominated by the ferroelectric material and the substantially superior performance achieved with PZT compared to $BaTiO_3$ *at the same electron density* supports the view that the ferroelectric's role is partially catalytic.

Formation of ammonia would then proceed via the reactions:

$$NH + H_2 \rightarrow NH_2 + H \quad (8)$$

$$NH_2 + H_2 \rightarrow NH_3 + H \quad (9)$$

and indeed these elementary steps are well established in the case of conventional heterogeneously-catalysed ammonia synthesis [2].

Given the relatively low strength of the N-H bond energy in NH_3 (385.53 kJ mol^{-1} [31]), another possible source of NH* species is the decomposition reaction:

$$NH_3 + e^- \rightarrow NH^* + 2\,H^* + e^- \quad (10)$$

Its relative importance will depend on the concentration of ammonia within the plasma volume and the residence time. Note also that the surface of the ferroelectric material could also contribute to ammonia decomposition.

4. Conclusions

A ferroelectrically-moderated DBD plasma provides an efficient method for the synthesis of ammonia under ambient conditions of temperature and pressure. The optimum operating conditions that maximize energy efficiency were achieved with PZT as the ferroelectric material and a large inter-electrode gap. The N_2 conversion achieved in the present work is superior to anything previously attained with H_2-N_2 plasmas. Comparison of the performances attained with PZT and with $BaTiO_3$ under conditions of similar electron density indicate that the ferroelectric material plays a catalytic as well as an electrical role. Analysis of the optical emission spectra and comparison with the corresponding ammonia production indicates that N_2^+ is the likely reaction initiating species. In addition to frequency and voltage, residence time is shown to be a key operational parameter, likely due to its effect on secondary reactions that lead to the subsequent destruction of initially formed NH_3. These encouraging results indicate avenues for further development.

Acknowledgments

We thank the Junta de Andalucía (Project P12-2265 MO) and the MINECO-CSIC (Project RECUPERA 2020) for financial support.

References

[1] Apply M 2006 Ammonia *Ullmann's Encyclopedia of Industrial Chemistry* (Weinheim: Wiley) pp 1–155
[2] Ertl G 2008 *Angew. Chem. Int. Ed.* **47** 3524
[3] Schlögl R 2008 *Handbook of Heterogeneous Catalysis* ed G Ertl *et al* (Weinheim: Wiley) p 2501
[4] Huo Y X, Wernick D G and Liao J C 2012 *Curr. Opin. Biotech.* **23** 406
[5] Hessel V, Anastasopoulou A, Wang Q, Kolb G and Lang J 2013 *Catal. Today* **211** 9
[6] Rafiqul I, Weber Ch, Lehmann B and Voss A 2005 *Energy* **30** 2487
[7] Sugiyama K, Akazawa K, Oshima M, Miura H, Matsuda T and Nomura O 1986 *Plasma Chem. Plasma Process.* **6** 179
[8] Nakajima J and Sekiguchi H 2008 *Thin Solid Films* **516** 4446
[9] Uyama H and Matsumoto O 1989 *Plasma Chem. Plasma Process.* **9** 421
[10] Uyama H and Matsumoto O 1989 *Plasma Chem. Plasma Process.* **9** 13
[11] Bai M, Zhang Z, Bai M, Bai X and Gao H 2008 *Plasma Chem. Plasma Process.* **28** 405
[12] Helden J H, Wagemans W, Yagci G, Zijlmans R A B, Schram D C, Engeln R A H, Lombardi G, Stancu G D and Röpcke J 2007 *J. Apply. Phys.* **101** 043305
[13] Mizushima T, Matsumoto K, Sugoh J, Ohkita H and Kakuta N 2004 *Appl. Catal. A Gen.* **265** 53
[14] Mizushima T, Matsumoto K, Ohkita H and Kakuta N 2007 *Plasma Chem. Plasma Process.* **27** 1
[15] Hong J, Prawer S and Murphy A B 2014 *IEEE Trans. Plasma Sci.* **42** 2338
[16] Bai M, Zhang Z, Bai X, Bai M and Ning W 2003 *IEEE Trans. Plasma Sci.* **31** 1285

[17] Gómez-Ramírez A, Rico V J, Cotrino J, González-Elipe A R and Lambert R M 2014 *ACS Catal.* **4** 402
[18] Rico V J, Hueso J L, Cotrino J and González-Elipe A R 2010 *J. Phys. Chem.* A **114** 4009
[19] Rico V J, Hueso J L, Cotrino J, Gallardo V, Sarmiento B, Brey J J and González-Elipe A R 2009 *Chem. Commun.* 6192
[20] Kang W S, Park J M, Kim Y and Hong S H 2003 *IEEE Trans. Plasma Sci.* **31** 504
[21] http://nl.lxcat.net/solvers/BOLSIG+/
[22] Manley T C 1943 *Trans. Electrochem. Soc.* **84** 83
[23] Montoro de Damas A M, Brey J J, Rodríguez M A, González-Elipe A R and Cotrino J *J. Power Sources* **296** 268
[24] Pearse R W B and Gaydon A G 1965 *The Identification of Molecular Spectra* (London: Chapman and Hall Ltd)
[25] Bibinov N K, Fateev A A and Wiesemann K 2001 *J. Phys. D: Appl. Phys.* **34** 1819
[26] http://physics.nist.gov/PhysRefData/Handbook/Tables/nitrogentable2.htm National Institute of Standard and Technology
[27] Kabbadj Y, Huet T R, Rehfuss B D, Gabrys C M and Oka T 1994 *J. Mol. Spectrosc.* **163** 180
[28] Yin K S and Venugopalan M 1983 *Plasma Chem. Plasma Process.* **3** 343
[29] Kiyooka H and Matsumoto O 1996 *Plasma Chem. Plasma Process.* **16** 547
[30] Nomura O 1983 *Technocrat* **16** 29
[31] Gibson S T, Greene J P and Berkowitz J 1985 *J. Chem. Phys.* **83** 4319